J|A|C|S
ARTICLES
Published on Web 03/18/2003

An Experimental and Theoretical Study of the ^{13}C and ^{31}P Chemical Shielding Tensors in Solid O-Phosphorylated Amino Acids

Marek J. Potrzebowski,[†] Xavier Assfeld,[‡] Katarzyna Ganicz,[†] Sebastian Olejniczak,[†] Alain Cartier,[‡] Carole Gardiennet,[§] and Piotr Tekely*,[§]

Contribution from the Polish Academy of Sciences, Centre of Molecular and Macromolecular Studies, 90-363 Łódź, Poland, and Université Henri Poincaré, Nancy 1, UMR CNRS 7565 and FRE CNRS 2415, 54506 Vandoeuvre-lès-Nancy, France

Received December 20, 2002; E-mail: piotr.tekely@rmn.uhp-nancy.fr

Abstract: A series of L and DL forms of O-phosphorylated amino acids (serine, threonine, tyrosine) have been studied by using solid-state multinuclear NMR spectroscopy and ab initio calculations. Principal elements of the ^{13}C and ^{31}P chemical shielding tensors have been measured and discussed in relation to zwitterionic structures and intermolecular contacts. DFT calculations have been compared with experimental data showing their ability to reproduce experimentally obtained tensor values in this challenging class of compounds. The changes of orientation of ^{31}P chemical shielding tensor with respect to the molecular frame in the presence of hydrogen bonds have been revealed and discussed on the ground of theoretical calculations. The measurements of internuclear P···P distances, based on Zeeman magnetization exchange betwen ^{31}P spins with differing chemical shielding tensor orientations, were exploited for a clear distinction between enantiomers and racemates.

Protein phosphorylation is of prime importance for enzymatic and cellular regulation.[1] Its mechanism controls protein structure, dynamics, and biological functions and plays a crucial role in metabolic pathways, kinase cascade activation, membrane transport, and gene transcription. The importance of these issues was reviewed very recently by several authors.[2,3]

Phosphorylation and dephosphorylation involve replacement of the hydroxyl group by a phosphate residue and vice versa in numerous biologically active compounds such as carbohydrates, nucleic acids, and proteins.[3] In enzymatic reactions, the transfer proceeds via phosphorylation of OH function of serine residue; however, the threonine and tyrosine can be also involved. The incorporation of the phosphate group in the polypeptide chain may change its conformation and mode of the intermolecular interactions, so any spectroscopic information, which sheds light on the structural properties of this class of compounds, is strongly desired. In fact, a broad range of analytical techniques, including NMR spectroscopy, was employed to investigate phosphoserine,[4] phosphothreonine,[5] and phosphotyrosine[6] in the liquid state.

In recent years, high-resolution solid-state NMR spectroscopy has become an attractive and powerful tool for investigation of biological samples. A number of papers, which employ NMR and discuss spectroscopic features of enantiomeric and racemic forms of amino acids, including leucine, methionine, selenomethionine, and aspartic acid, have been published.[7−13]

Moreover, some aspects of the relationship between ^{13}C and ^{15}N principal elements of chemical shift tensors and the strength of hydrogen bonds in peptides and amino acids were discussed in the literature.[14−18] Hydrogen bonding was shown to have a

[†] Polish Academy of Sciences.
[‡] Chimie Théorique, Université Henri Poincaré.
[§] Méthodologie RMN, Université Henri Poincaré.

(1) Corbridge, D. E. C. In *Phosphorus, An Outline of its Chemistry, Biochemistry and Technology*, 4th ed.; Elsevier: Amsterdam-Oxford-New York-Tokyo, 1990; Chapter 13, pp 880−956.
(2) Johnson, L. N.; Lewis, R. J. *Chem. Rev.* **2001**, *101*, 2209. Jones S. M.; Kazlauskaz, A. *Chem. Rev.* **2001**, *101*, 2413. Bridges, A. J. *Chem. Rev.* **2001**, *101*, 2541. Majeti, R.; Weiss, A. *Chem. Rev.* **2001**, *101*, 2441.
(3) Haskell, M. D.; Slack, J. K.; Parsons, T.; Parsons, S. J. *Chem. Rev.* **2001**, *101*, 2425. Saito, H. *Chem. Rev.* **2001**, *101*, 2497. Ali, A.; Hoeflich, K. P.; Woodgett, J. R. *Chem. Rev.* **2001**, *101*, 2527.
(4) Arnold, L. D.; May, R. G.; Vederas, J. C. *J. Am. Chem. Soc.* **1988**, *110*, 2237.
(5) Robitaille, P. M. L.; Robitaille, P. A.; Brown, G. G. *J. Magn. Reson.* **1991**, *92*, 73.
(6) Alewood, P. F.; Johns, R. B.; Valerio, R. M. *Synthesis* **1983**, *1*, 30. Lee, T. R.; Mendelow, M.; Srinivasan, J.; Kwon, Y. G.; Lawrence, D. S. *J. Am. Chem. Soc.* **1993**, *115*, 9888.
(7) Keniry, M. A.; Rothgeb, T. M.; Smith, R. L.; Gutowsky, H. S.; Oldfield, E. *Biochemistry* **1983**, *22*, 1917.
(8) Diaz, L. E.; Morin, F.; Mayne, C. L.; Grant D. M.; Chang, C. J. *Magn. Reson. Chem.* **1986**, *24*, 167.
(9) Gu, Z.; Ebisawa, K.; McDermott, A. *Solid State Nucl. Magn. Reson.* **1996**, *7*, 161.
(10) Frey, M. H.; Opella S. J. *J. Chem. Soc., Chem. Commun.* **1980**, 474.
(11) Hollingsworth, M. D.; Cyr, N. *J. Chem. Soc., Chem. Commun.* **1990**, 578.
(12) Belton, P. S.; Gil, A. M.; Tanner, S. F. *Solid State Nucl. Magn. Reson.* **1992**, *1*, 67.
(13) Potrzebowski, M. J.; Katarzynski R.; Ciesielski, W. *Magn. Reson. Chem.* **1999**, *37*, 173.
(14) Ando, S.; Ando, I.; Shoji, A.; Ozaki, T. *J. Am. Chem. Soc.* **1988**, *110*, 3380.
(15) Gu, Z.; Zambrano, R.; McDermott, A. *J. Am. Chem. Soc.* **1994**, *116*, 6368.
(16) Wei, Y.; de Dios, A. C.; McDermott, A. E. *J. Am. Chem. Soc.* **1999**, *121*, 10389.
(17) (a) Sitkoff, D.; Case D. A. *Prog. Nucl. Magn. Reson. Spectrosc.* **1998**, *32*, 165−190. (b) Antzutkin, O. N., *Molecular Structure Determination: Application in Biology*. In *Solid State NMR spectroscopy principles and applications*; Duer, M. J., Ed.; Blackwell Science: 2002; Chapter 7, pp 280−390.

Chart 1

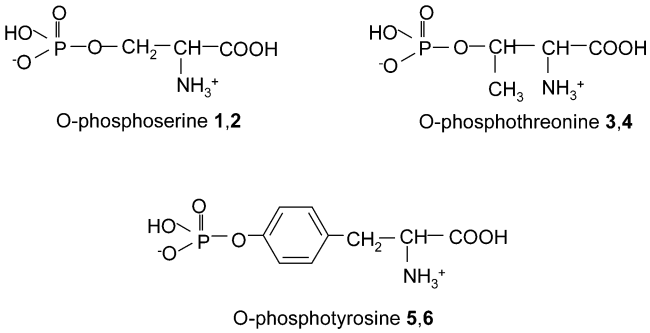

negligible effect on the orientation of the ^{15}N chemical shift tensor in peptide.[18b] However, there are, to our knowledge, no solid-state NMR reports to unambiguously interpret variations in chemical shift anisotropy (CSA) parameters in terms of the type of hydrogen bonding or three-dimensional structure. Moreover, the O-phosphorylated amino acids, despite their importance in enzymatic chemistry, have not been systematically investigated by high-resolution solid-state NMR.

In this work we report ^1H, ^{13}C, and ^{31}P solid-state NMR and the density functional theory (DFT) studies of O-phosphorylated serine, threonine, and tyrosine (Chart 1). The main aims of our work are to characterize the ^{13}C and ^{31}P principal elements of chemical shift tensors and to probe the dependence of magnetic shielding on the geometrical configuration of the hydrogen bond pattern. Hydrogen bonding is the most important of all directional intermolecular interactions.[19] Correlation of such contacts with the spectroscopic response is still very challenging for solid-state NMR.

Very recently, some of us have reported[20,21] the measurements of internuclear distances between chemically equivalent nuclei in single ^{13}C-labeled model compounds of biological interest by using the ODESSA method.[22] Here, employing L and DL O-phosphorylated amino acids, we demonstrate that this approach is also a powerful tool for a clear distinction between enantiomers and racemates and or an unambiguous recognition of distinctinternuclear P····P distances. The method is based on the fact that molecular symmetries and packing of enantiomers and racemates are significantly different.

Experimental Section

Materials. All of the O-phosphorylated amino acids were purchased from Sigma-Aldrich and used without further purification. Sundaralingam and Putkey[23,24] reported the X-ray data for *O*-phospho-L-serine **1** and *O*-phospho-DL-serine **2** which crystallize in the space group $P2_12_12_1$ and $C2/c$, respectively. The structure of *O*-phospho-L-threonine **3** and O-phospho-DL-threonine **4** have been reported by Maniukiewicz et al.[25] Crystals of **3** are orthorhombic and the space group is $P2_12_12_1$ while compound **4** crystallizes in the space group $P2_1/c$. The crystal structure of *O*-phospho-L-tyrosine **5** has been reported very recently by Suga and co-workers.[26] This compound crystallizes in the monoclinic space group $P2_1$ with two conformers present in the asymmetric unit cell. The compounds **1**−**5** form zwitterionic structures. The amino groups and phosphate residues are charged but the carboxyl groups are not. This feature distinguishes phosphorylated amino acids from native amino acids where the carboxyl group is in an ionic form.[15]

Solid-State NMR Experiments. All experiments were carried out using BRUKER Avance-300 and 400 NMR spectrometers. A 7 mm double resonance magic-angle spinning (MAS) probe tuned to ^{13}C and ^{31}P frequencies at 75.46 and 121.46 MHz, respectively, was used. The CP/MAS NMR spectra were recorded in the presence of phase-inversion (PI) high-power proton decoupling.[27] The ^{13}C chemical shifts were measured indirectly by reference to the carbonyl α-glycine line set at 176.5 ppm, and the ^{31}P chemical shifts were calibrated indirectly through bis(dineopentoxyphosphorothioyl) disulfide set at 84.0 ppm. The principal components δ_{ii} of CSA tensors were derived from low-speed MAS one and/or two-dimensional spectra and used for calculation of anisotropy $\Delta\delta$, asymmetry η, span Ω, and skew κ parameters. For ^1H MAS experiments at 400.13 MHz, a 2.5 mm rotor was used and sample was spun at 32 kHz.

Computational Details. All calculations have been carried out with the quantum chemistry package Gaussian98.[28] The density functional theory (DFT) method used is the hybrid functional B3[29] for the electronic quantum exchange and LYP for the electronic correlation,[30] since it had been shown to produce reliable data at least for carbon atom.[31] Shielding constant tensors are evaluated by using the GIAO formalism.[32]

Results

^1H High-Speed MAS NMR Spectra. Recent progress in the design of commercially available MAS probes allows for spinning frequencies up to 35 kHz. In solids with not very tightly coupled protons, such spinning frequencies are sufficient to remove efficiently the dipolar broadening, which results in highly resolved proton spectra. This permits one to obtain straightforward information about the strength of hydrogen bonding from a single pulse, proton magic-angle spinning spectra. Figure 1 shows ^1H MAS spectra of **1**−**6** compounds with an efficient narrowing of the dipolar broadening, permitting a clear resolution of isotropic positions representing different types of functional groups, non-hydrogen-bonded CH_3, CH_2, CH, and aromatic protons appearing about 1.8−1.9 ppm, 4.0−4.5 ppm, 5.1−5.2 ppm, and 6.6−7.0 ppm, respectively, along with hydrogen-bonded NH_3, COOH, and POOOH protons showing up between 8.0 and 16.8 ppm.

(18) (a) Wei, Y.; Lee, D.-K.; Ramamoorthy, A. *J. Am. Chem. Soc.* **2001**, *123*, 6118. (b) Brender, J. R.; Taylor, D. M.; Ramamoorthy, A. *J. Am. Chem. Soc.* **2001**, *123*, 914. (c) Lee, D.-K.; Wei, Y.; Ramamoorthy, A. *J. Phys. Chem. B* **2001**, *105*, 4752.
(19) Steiner, T. *Angew. Chem., Int. Ed.* **2002**, *41*, 48−76.
(20) (a) Tekely, P.; Potrzebowski, M. J.; Dusausoy Y.; Luz Z. *Chem. Phys. Lett.* **1998**, *291*, 471. (b) Potrzebowski, M. J.; Schneider, C.; Tekely, P. *Chem. Phys. Lett.* **1999**, *313*, 569−574.
(21) Tekely, P.; Gardiennet, C.; Potrzebowski, M. J.; Sebald, A.; Reichert, D.; Luz, Z. *J. Chem. Phys.* **2002,** *116*, 7607.
(22) Gérardy-Montouillout, V.; Malveau, C.; Tekely, P.; Olender Z.; Luz Z. *J. Magn. Reson. A* **1996**, *123*, 7.
(23) Sundaralingam, M.; Putkey, E. F. *Acta Cryst*. **1970**, *B26*, 790.
(24) Putkey, E. F.; Sundaralingam, M. *Acta Crystallogr*. **1970**, *B26*, 782.
(25) Maniukiewicz, W.; Kwiatkowski, W.; Blessing, R. H. *Acta Crystallogr*. **1996**, *C52*, 1736.
(26) Suga, T.; Inubushi, C.; Okabe, N. *Acta Crystallogr*. **1998**, *C54*, 83.
(27) Tekely, P.; Palmas P.; Canet, D. *J. Magn. Reson. A* **1994**, *107*, 129.
(28) Frisch, M. J.; Trucks, G. W.; Schlegel, H. B.; Scuseria, G. E.; Robb, M. A.; Cheeseman, J. R.; Zakrzewski, V. G.; Montgomery, Jr., J. A.; Stratmann, R. E.; Burant, J. C.; Dapprich, S.; Millam, J. M.; Daniels, A. D.; Kudin, K. N.; Strain, M. C.; Farkas, O.; Tomasi, J.; Barone, V.; Cossi, M.; Cammi, R.; Mennucci, B.; Pomelli, C.; Adamo, C.; Clifford, S.; Ochterski, J.; Petersson, G. A.; Ayala, P. Y.; Cui, Q.; Morokuma, K.; Malick, D. K.; Rabuck, A. D.; Raghavachari, K.; Foresman, J. B.; Cioslowski, J.; Ortiz, J. V.; Baboul, A. G.; Stefanov, B. B.; Liu, G.; Liashenko, A.; Piskorz, P.; Komaromi, I.; Gomperts, R.; Martin, R. L.; Fox, D. J.; Keith, T.; Al-Laham, M. A.; Peng, C. Y.; Nanayakkara, A.; Gonzalez, C.; Challacombe, M.; Gill, P. M. W.; Johnson, B.; Chen, W.; Wong, M. W.; Andres, J. L.; Gonzalez, C.; Head-Gordon, M.; Replogle, E. S.; Pople, J. A. *Gaussian 98*, Revision A.7; Gaussian, Inc.: Pittsburgh, PA, 1998.
(29) Becke, A. D. *J. Chem. Phys.* **1993**, *98***,** 5648.
(30) Lee, C.; Yang, W.; Parr, R. G. *Phys. Rev. B* **1988**, *37***,** 785.
(31) (a) Helgaker, T.; Jaszunski, M.; Ruud, K. *Chem. Rev.* **1999**, *99*, 293. (b) Rich, J. E.; Manalo, M. N.; de Dios, A. C. *J. Phys. Chem. A* **2000**, *104*, 5837.
(32) (a) Ditchfield, R. *Mol. Phys.* **1974**, *27*, 789. (b) Wolinski, K.; Hinton J. F.; Pulay, P. *J. Am. Chem. Soc.* **1990**, *112*, 8251.

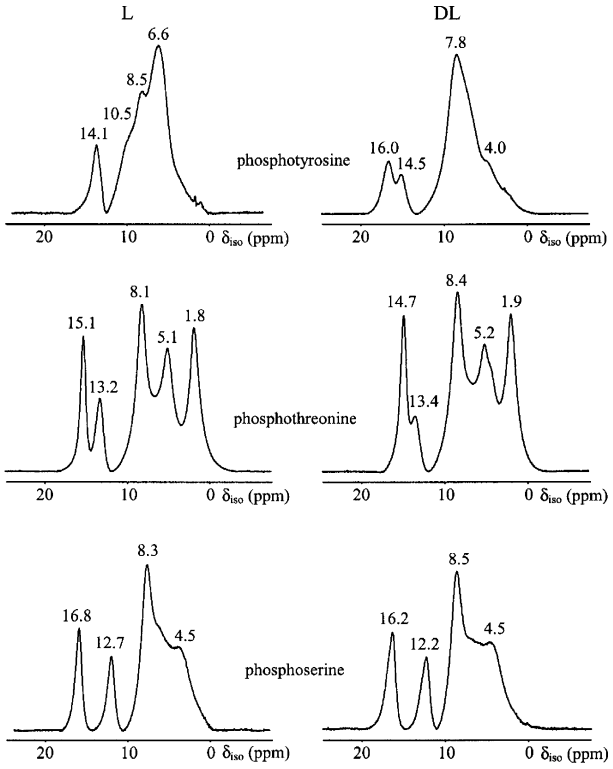

Figure 1. ^{1}H MAS spectra of O-phosphorylated amino acids recorded at 400.13 MHz and a spinning rate of 32 kHz.

Proton NMR spectroscopy, a sensitive probe of the hydrogen environment, has been widely utilized to investigate the nature of hydrogen bond systems of biological interest.[33] A large range of proton NMR chemical shifts of ca. 20 ppm is observed in solids for oxygen-bound hydrogens. Berglund and Vaughan reported the correlation between ^{1}H chemical shift and O···O distances.[34] Harris et al. investigated the organic derivatives of carboxylic and phosphoric acids by means of combined rotation and multiple pulse methodology (CRAMPS).[35]

The hydrogen bond distances in O-phosphorylated amino acids **1**−**5** were reported in papers dealing with the X-ray analysis of these compounds. In each case, the hydrogen bond network involves the phosphate, carboxyl, and amino groups. For example, in the case of **1**,[23] besides a very short hydrogen bond between the phosphate oxygen atom and the carboxyl hydroxyl oxygen atom (2.477 Å), the shortest hydrogen bond between phosphate groups is 2.547 Å. Consequently, we assign the ^{1}H signals at 16.8 and 12.7 ppm to the P−O···H−O−C and P−O···H−O−P hydrogen bonds, respectively. Longer hydrogen bonds are represented by ^{1}H resonance signals between 8 and 9 ppm and have to involve the protonated amino group: the two shorter, 2.780 and 2.786 Å, are with two different phosphate groups and the third, 2.953 Å, is with the carboxyl hydroxyl group.[23] Table 1 summarizes the shortest hydrogen bond distances in O-phosphorylated amino acids.

The data indicate that shortest hydrogen bond distances in L forms of phosphorylated amino acids are systematically those involving the carboxyl group; a reverse situation takes place in the DL form of serine and threonine. On the basis of linear correlations shown in Figure 2, the corresponding distances of 2.48 ± 0.02 and 2.55 ± 0.02 Å for P−O···H−O−P and P−O···H−O−C groups in DL phosphotyrosine have been estimated (dashed lines).

Table 1. Shortest Hydrogen Bond Distances (Å) in L and DL Crystals of O-Phosphorylated Amino Acids

D′-D-H···A-A′	H···A	D···A	ref
O-phospho-L-serine			25
P−O3−H3···O1 P	1.63	2.55	
C−O−H···O2 P	1.53	2.48	
O-phospho-DL-serine			25
P−O2···H···O2 P	1.56	2.49	
P−O3···H···O3 P	1.55	2.49	
C−O−H···O2 P	1.64	2.59	
O-phospho-L-threonine			25
P−O3−H3···O1 P	1.63	2.53	
C−O−H···O2 P	1.62	2.53	
O-phospho-DL-threonine			25
P−O3−H3···O1 P	1.63	2.54	
C−O−H···O2 P	1.64	2.59	
O-phospho-L-tyrosine			26
P−O3−H3···O1 P	1.66	2.65	
C−O−H···O2−P	1.58	2.58	this work
O-phospho-DL-tyrosine		2.48	
P−O3−H3···O1−P		2.55	
C−O−H···O2−P			

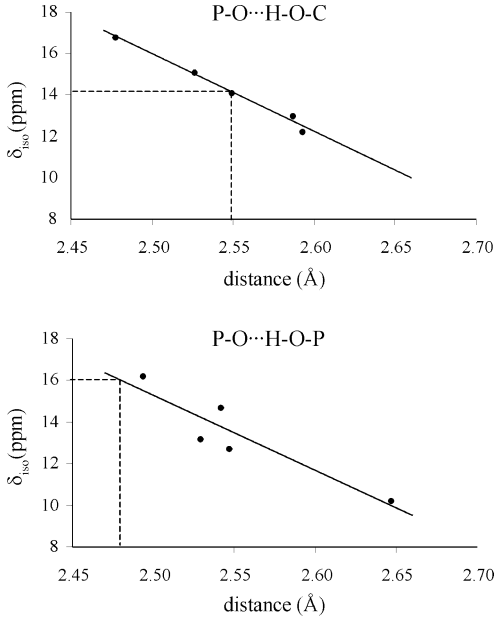

Figure 2. Plots of isotropic ^{1}H chemical shifts versus P−O···H−O−C and P−O···H−O−P hydrogen bond lengths.

^{13}C NMR Data. For rotating solids, the principal components δ_{ii} of chemical shift tensors are available from the analysis of spinning sidebands resulting from the modulation of chemical shift anisotropy interaction by macroscopic rotation. For compounds **1**−**4**, the principal values of the carboxyl tensor can be extracted easily from low-speed 1D CP/MAS spectra.

For **5** and **6**, due to the overlap of spinning sidebands from carboxyl and aromatic carbons, the separation of isotropic and anisotropic part of chemical shift effects in the two-dimensional manner was necessary. Among several approaches, which allow achieving such a goal, we have chosen the PASS (phase-adjusted spinning sidebands) 2D method,[36] which compared to other methods offers a good sensitivity and does not require any hardware modifications or special probehead.

(33) Brown, S. P.; Spiess, H. W. *Chem. Rev.* **2001**, *101*, 4125−4155.
(34) Berglund, B.; Vaughan, R. W. *J. Chem. Phys.* **1980**, *73*, 2037.
(35) Harris, R. K.; Jackson, P.; Merwin, L. H.; Say, B. J.; Haegelle G. *J. Chem. Soc., Faraday Trans.* **1988**, *84*, 3649.

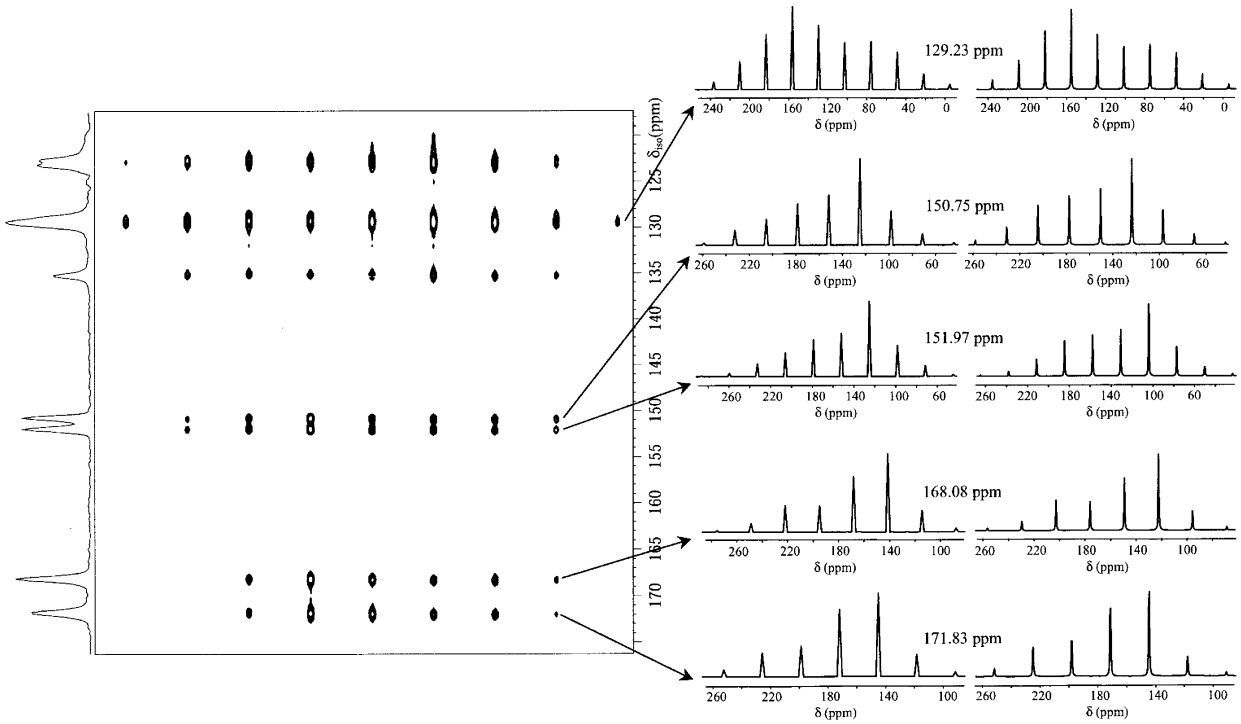

Figure 3. 2D-PASS spectrum of *O*-phospho-L-tyrosine **5**, recorded at a spinning frequency of 2 kHz, along with the experimental (left) and the best-fitting simulated (right) manifolds of CSA spinning sidebands.

Table 2. Experimental ^{13}C and ^{31}P Values of the Principal Tensor Elements δ_{ii} and Corresponding Anisotropic Parameters for O-Phosphorylated Amino Acids **1**−**6**[a] (^{13}C Data for α and β Carbons Are Omitted)

^{13}C NMR Data

O-phosphorylated amino acid	δ_{iso} (ppm)	δ_{11} (ppm)	δ_{22} (ppm)	δ_{33} (ppm)	$\lvert\Delta\delta\rvert$ (ppm)	Ω (ppm)	η	κ
L-serine	171.0	247	152	111	114	136	0.54	−0.42
DL-serine	169.3	251	153	104	122	147	0.60	−0.33
L-threonine	172.0	244	163	109	108	135	0.75	−0.20
DL-threonine	173.0	246	164	109	110	137	0.75	−0.20
L-tyrosine A	171.3	247	150	116	114	131	0.45	−0.49
B	167.7	252	137	114	126	138	0.27	−0.67
A	151.5	256	138	60	157	196	0.75	−0.21
B	150.3	247	133	71	145	176	0.64	−0.29
	128.9	232	149	5	186	227	0.67	0.27
DL-tyrosine	170.9	248	156	109	112	134	0.61	−0.33
	149.7	239	133	76	134	163	0.64	−0.31
	130.4	226	148	17	170	209	0.69	0.25

^{31}P NMR Data

O-phosphorylated amino acid	δ_{iso} (ppm)	δ_{11} (ppm)	δ_{22} (ppm)	δ_{33} (ppm)	$\lvert\Delta\delta\rvert$ (ppm)	Ω (ppm)	η	κ
L-serine	−0.9	51	4	−57	84.5	108	0.83	0.14
DL-serine	1.9	54	6	−54	84.0	108	0.86	0.11
L-threonine	−3.7	56	5	−72	102.5	128	0.75	0.20
DL-threonine	−0.9	51	5	−58	86.0	109	0.81	0.16
L-tyrosine	−4.3	66	7	−86	122.5	152	0.72	0.22
	−5.9	61	3	−82	114.0	143	0.76	0.19
DL-tyrosine	−3.3	60	−7	−63	95.0	123	0.88	−0.09

[a] Estimated errors in δ_{11}, δ_{22}, and δ_{33}, are ±3 ppm; span is expressed as $\Omega = \delta_{11} - \delta_{33}$, skew as $\kappa = 3(\delta_{22} - \delta_{iso})/\Omega$; anisotropy is calculated as $\Delta\delta = 3/2(\delta_{33} - \delta_{iso})$ and asymmetry as $\eta = (\delta_{22} - \delta_{11})/(\delta_{33} - \delta_{iso})$ when $|\delta_{11} - \delta_{iso}| \leq |\delta_{33} - \delta_{iso}|$ or as $\Delta\delta = 3/2(\delta_{11} - \delta_{iso})$ and $\eta = (\delta_{22} - \delta_{33})/(\delta_{11} - \delta_{iso})$ when $|\delta_{11} - \delta_{iso}| \geq |\delta_{33} - \delta_{iso}|$.

Figure 3 displays the PASS-2D spectrum of *O*-phospho-L-tyrosine **5**, recorded at the spinning frequency of 2 kHz. The unit cell of this compound contains two molecules; therefore 18 resonance peaks can be expected in the isotropic dimension. However, some of the aromatic signals are isochronous so only 11 resonances were monitored. As shown in Figure 3, proper data shearing permits the separation of the spinning sideband manifold for each carbon which opens the way to simulations of individual CSA parameters. With the exception of the α and β carbons, the ^{13}C isotropic chemical shifts and the fitted values of the principal tensor element δ_{ii} along with the anisotropic parameters are given for compounds **1** to **6** in Table 2.

^{31}P NMR Data. So far, only ^{31}P NMR parameters of *O*-phospho-L-serine **1** have been reported.[37] Both powder and

(36) Antzutkin, O. N.; Shekar, S. C.; Levitt, M. H. *J. Magn. Reson.* **1995**, *115*, 7. Antzutkin, O. N.; Lee, Y. K.; Levitt, M. H. *J. Magn. Reson.* **1998**, *135*, 144.
(37) Kohler S. J.; Klein, M. P. *J. Am. Chem. Soc.* **1977**, *99*, 8290.

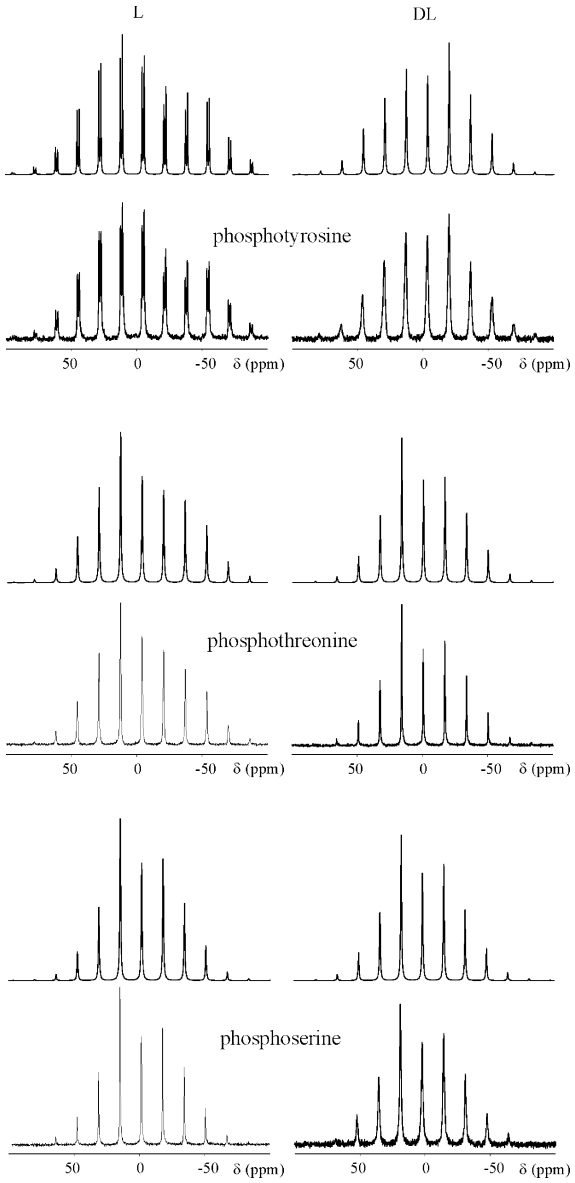

Figure 4. Experimental and the best-fitting simulated manifolds of ^{31}P CSA spinning sidebands of L (left) and DL forms (right) of O-phosphorylated serine (bottom), threonine (center), and tyrosine (top). The spinning frequency was 1.4 kHz.

single crystal of **1** were investigated. The ^{31}P δ_{ii} parameters for the powdered sample were found to be 59, −4, and −53 ppm. Figure 4 shows ^{31}P CP/MAS (CT = 1 ms) experimental and corresponding fitted spectra of **1**−**6**. The ^{31}P isotropic chemical shifts and the fitted values of the principal tensor elements δ_{ii} along with corresponding anisotropic parameters are given in Table 2.

The dependence of the spin-diffusion rate constants upon the inverse sixth power of the internuclear distances between the participating spins makes information about the spatial arrangement of the involved spins available from the polarization-transfer rate constants between specific sites.[38] Zeeman magnetization exchange between ^{13}C spins with identical isotropic chemical shifts but differing ^{13}C chemical shielding tensor orientations may be measured using the ODESSA experiment,[22] and the spin-diffusion rate constants derived from this experiment provide a route to internuclear distance.[20,21] The ODESSA experiment is a rotor-synchronized MAS NMR exchange experiment with the preparation period fixed to one-half of a rotation period, $\tau_1 = \tau_r/2$, and the mixing time τ_m equal to an integer number of rotation periods, $\tau_m = N\tau_r$. This experiment ensures that at the beginning of the mixing time the magnetization associated with the various spinning sidebands is polarized in alternate directions. Due to the fact that crystallites with different orientations contribute differently to different spinning sidebands, an initial state is prepared where the level populations of the nuclear spins are disturbed nonuniformly and spin exchange results in a redistribution of polarization and a corresponding change in the spinning sidebands intensities.

Figure 5 shows the ^{31}P proton-driven (occurring in the absence of proton decoupling during the mixing time) ODESSA decays for compounds **1**−**6**, with each plot representing a normalized total spectral intensity as a function of the mixing time τ_m. In all cases, a function of the type $f(\tau_m) = A\exp(-W'\tau_m) + B\exp(-W''\tau_m)$ has been used to fit the experimental data. Although the experimental decays can be fitted satisfactorily to a single exponential, the biexponential function $f(\tau_m)$ has the advantage of perfectly fitting the long-time changes which seem to account for spin exchange between more distant nuclei and for possible different rate constants of differently oriented pairs of spins. Due to very long T_1 relaxation times, of the order of several tens of seconds, all decays are practically insensitive to longitudinal relaxation and are essentially determined by the exchange rate constant W'.

Ab Initio Calculations of NMR Shielding Parameters. To check that the calculated values have reached a required convergence with respect to the one-electron basis set size, various basis functions were tested on compound **1** by taking its solid-state geometry and going from 6-31G up to 6-311++G-(3df,3pd) (see also Supporting Information). On the basis of these preliminary results, and in order to keep the computational parameters (CPU time and disk storage) to reasonable limits and to maintain the average error about 10 ppm for P atom and about 1 ppm for C atom, the 6-311++G** basis set has been chosen throughout the remaining part of this work. The hydrogen atom bond lengths have been optimized with the PM3[46a,b] semiempirical Hamiltonian keeping fixed orientations from the crystallographic data as imposed by the network of hydrogen bonds.

Two types of calculations have been considered. The first one is performed on an isolated molecule, and uses the solid-state geometry as revealed by X-ray studies.[39] The second type is carried out on the model of the crystal. Consequently, any variation in results obtained from these two types of computation will reflect the electronic polarization. A computational model to describe the crystal is presented in the next section. One has to note that all calculations have been performed for zwitterionic isomers. Two main approaches are generally employed to evaluate shielding tensors for condensed chemical systems. The first approach takes a single molecule for quantum mechanics description, while the remaining molecules of the solid are taken into account by a set of atomic point charges. This has been developed by Pulay et al.[32,40] and successfully applied by de

(38) Suter, D.; Ernst, R. R. *Phys. Rev. B* **1985**, *32*, 5608.

(39) The experimental geometry was retrieved from the Centre for Molecular and Biomolecular Informatics facilities, University of Nijmegen, and Biomolecular Informatics facilities, University of Nijmegen, The Netherlands.

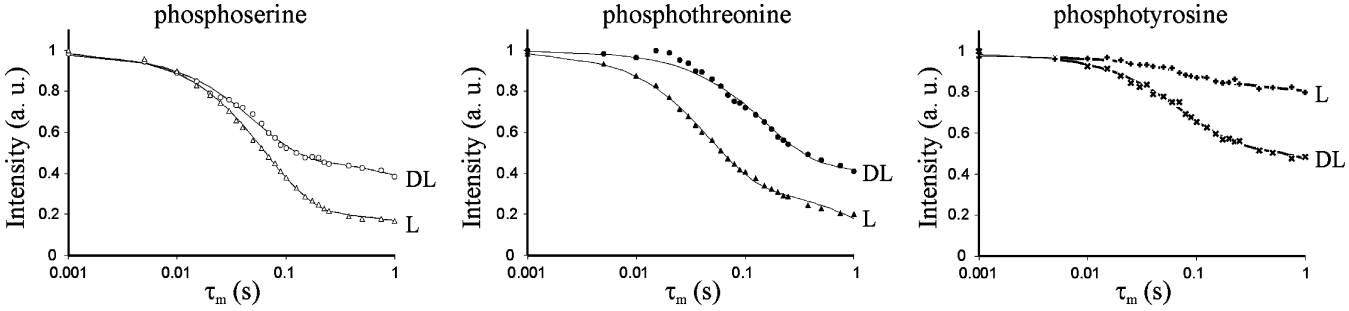

Figure 5. Evolution of the proton-driven ^{31}P magnetization exchange of O-phosphorylated amino acids in the ODESSA experiment.

Dios et al.[41] We wish to point out that although only the electrostatic interactions are taken into account by this approach, an acceptable agreement between computed and experimental data has been obtained for the ^{13}C shielding tensor of L-threonine and L-tyrosine in the solid state.[41b] Very recently, this approach has been refined by Grant and co-workers,[42] using a self-consistent iterative procedure to determine the set of atomic point charges. In the second approach, one can consider a small part of the solid, for example, a cluster of few molecules, and describe it by means of quantum chemistry tools. Although the long-range electrostatic interactions are neglected is this approach, all other intermolecular interactions can be taken into account, depending on the level of theory. Basically, charge transfer interactions are adequately defined in this manner which is an important advantage in the case of hydrogen-bonded systems. It is noteworthy that such an approach has also been used to compute the ^{15}N chemical shift anisotropy of hydrogen-bonded histidine.[16] Since the systems we are studying involve hydrogen-bonded zwitterionic molecules, the shielding tensors are mainly modified by the electrostatic and charge-transfer interactions. To probe the hierarchy of both contributions, we have tested both approaches on compound **1**. In the first approach, a cube of $5 \times 5 \times 5$ unit cells from the whole crystal was generated by the Madewa package.[43] A single molecule of the central cell was described quantum mechanically, and the remaining atoms were represented as point charges. Two sets of point charges were used: Mulliken atomic charges,[44] or CHELPG charges (atomic charges fitted to reproduce the electrostatic potential), both obtained at the B3LYP/6-311++G** level of theory.[45] In the case of the second approach, the cluster was defined as follows: the crystal was generated by symmetry operations of the corresponding space group and the X-ray crystallographic coordinates. All molecules, which are hydrogen-bonded to the carboxylic or phosphate group of the molecule of interest, were considered. In practice, to keep the computational time within reasonable limits, only the functional groups effectively hydrogen-bonded were taken into account. In this manner, the $R-NH_3^+$ group was modeled by the NH_4^+ molecule, the R−COOH group by the HCOOH molecule, and the $R-OPO_3H^-$ group by the $HOPO_3H^-$ ion. The position of substituting hydrogen atoms was optimized at the PM3 semiempirical level of theory,[46a,b] by assuming that the substitution occurred along the replaced chemical bond. The positions of all remaining atoms were kept frozen during this optimization. To make the discussion and the comparison of theoretical and experimental data easy, the shielding constants were converted into the chemical shifts. For the carbon atom, the isotropic shielding of TMS is found to be 184.1 ppm, at the B3LYP/6-311++G** level of theory. For the phosphorus atom, the isotropic shielding of PH_3 equals 525.3 ppm at the same level of theory. If we know the experimental chemical shift of PH_3 (−238 ppm),[46c] the absolute isotropic shielding of 85%$H_3PO_{4(aq)}$ is equal to 287.3 ppm.

Table 3. Principal Components (in ppm) of ^{13}C and ^{31}P CSA Tensors of Carboxyl Carbon and Phosphorus Atom in *O*-Phospho-L-serine Calculated for Various Models of the Solid Phase

	C			P		
model	δ_{11}	δ_{22}	δ_{33}	δ_{11}	δ_{22}	δ_{33}
Mulliken point charges	200.8	129.1	34.4	75.3	7.9	−209.3
ChelpG point charges	155.4	103.9	−62.5	62.6	32.2	−181.4
cluster	273.6	146.5	106.6	43.1	−21.3	−79.1
NMR experiment	247	152	111	51	4	−57

The results are presented in Table 3 and clearly show that the model of atomic point charges fails completely in reproducing experimental data. This is especially true in the case of phosphorus atoms and must be due to the lack of formalism describing electron transfer through hydrogen bonding. Consequently, we have proceeded further by using only the cluster approach.

Discussion

^{13}C and ^{31}P Chemical Shielding Tensors: Experiment versus Theory. Since one of the main goals in this work is to probe to what extent does hydrogen bonding influence NMR shielding parameters of the phosphorylated amino acids, we need first to assess the quality of our theoretical approach. This depends critically on the proper representation of zwitterionic isomers in the solid phase. The graphs of the theoretical ^{13}C and ^{31}P chemical shielding tensor elements plotted versus the experimentally determined chemical shift tensor principal values for isolated molecule and cluster type calculations are shown in Figures 6 and 7. Comparing the regression curve slopes for ^{31}P, which range from −2.091 to −1.154 (versus the ideal value of −1.0), we can see that the agreement between theory and experiment is dramatically improved by the cluster type calculation. Although for the carboxylic carbon the improvement

(40) Pulay, P.; Wolinski, K.; Hinton, J. F. *The Texas Program*; University of Arkansas, Fayetteville, AR, 1991.
(41) (a) De Dios, A. C.; Oldfield, E. *Chem. Phys. Lett.* **1993**, *205*, 108. (b) de Dios, A. C.; Laws, D. D.; Oldfield, E. *J. Am. Chem. Soc.* **1994**, *116*, 7784.
(42) Stueber, D.; Guenneau, F. N.; Grant, D. M. *J. Chem. Phys.* **2001**, *114*, 9236.
(43) Angyan, J.; Ferenczy, G.; Nortier, P. Madewa 1.0, 1996.
(44) Mulliken, R. S. *J. Chim. Phys.* **1949**, *46*, 497.
(45) Breneman, C. M.; Wiberg, K. B. *J. Comput. Chem.* **1990**, *11*, 361.

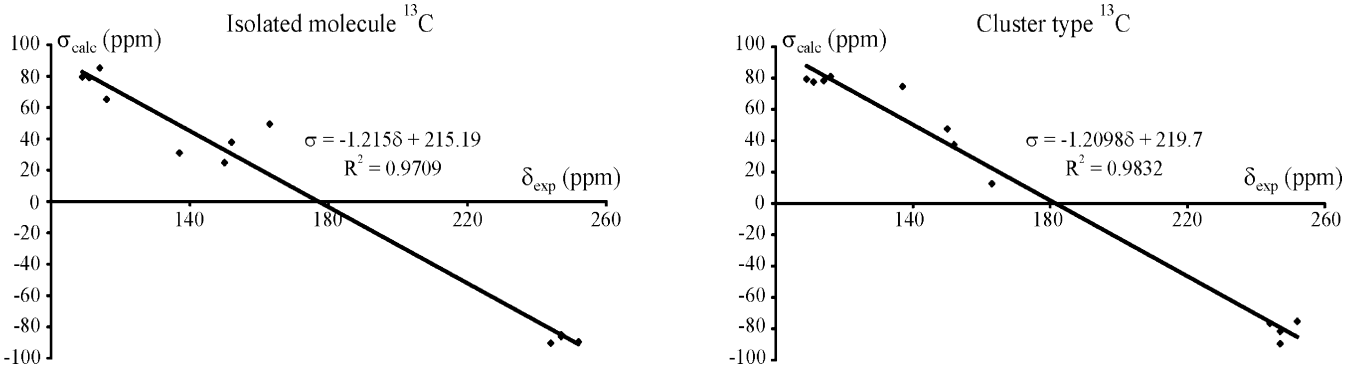

Figure 6. Calculated shielding parameters versus experimental chemical shifts of ^{13}C carboxylic atom of compounds **1**, **3**, and **5** (both conformers), as isolated molecules or as part of the hydrogen-bonded cluster.

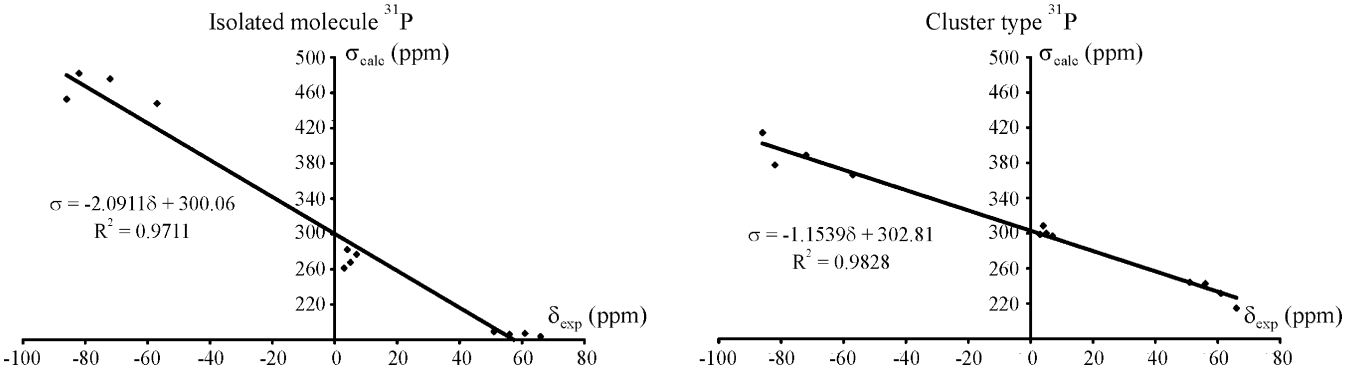

Figure 7. Calculated shielding parameters versus experimental chemical shifts of the ^{31}P atom of compounds **1**, **3**, and **5** (both conformers), as isolated molecules or as part of the hydrogen-bonded cluster.

is rather small, a better alignment of the middle tensor elements with the regression curve is clearly visible (R^2 value of 0.983 versus 0.971) when hydrogen bonds are considered. We anticipate that by using a higher level of theory (more complete basis set) and by taking into account the long-range electrostatic interactions, we would even improve the agreement. However, for the purpose of our work, we consider that the approach we used is satisfactory in describing the effect of hydrogen bonding. The comparison of the calculated chemical shielding elements (after conversion from σ to δ scale) with the experimental values is given in Table 4.

Much attention has been given to measuring the CSA tensors of carboxyl groups in peptides and amino acids. A strong dependence of the ^{13}C δ_{22} element on the hydrogen bond distance for the protonated and deprotonated forms has been reported by McDermott and co-workers.[15] As mentioned before, the carboxyl groups in the phosphorylated amino acids, contrary to the native amino acid analogues, are protonated. This feature is clearly recognized in the case of serine and tyrosine by distinct δ_{11} and δ_{22} components as compared with data for native amino acids. In fact, the values δ_{11} of 247−251 and 247−248 ppm and the values δ_{22} of 152−153 and 137−156 pmm have been found for **1**−**2** and **5**−**6**, respectively, while those reported for native serine and tyrosine were 242, 238, 174 and 184 ppm, respectively.[15,18,47,48] However, in the case of compounds **3**−**4**, the measured values of 244−246 ppm for δ_{11} and 163−164 ppm for δ_{22} are very similar to the values of 243−247 ppm and of 168 ppm, respectively, as reported for native threonine.[15,48] This would suggest a deprotonated character of carboxyl groups or the involvement of their protons in stronger hydrogen bonds. Indeed, the apparently deprotonated character in compounds **3**−**4** has to result from the involvement of the C═O group in a relatively strong and unique C═O···H−N hydrogen bonding (O···H−N of 2.86 and 2.92 Å) as compared with C−(H)−O···H−N hydrogen bonding (O···H−N of 2.95 and 3.11 Å)[25] in compounds **1**−**2** (there is no hydrogen bonding of this type in **5**−**6**). Such a feature of carboxyl carbons in phosphorylated threonines is especially clearly visualized in Table 2 by an important decrease of their skew values reflecting a more isotropic character of electronic distribution in the presence of two hydrogen bonds involving two different carboxyl oxygens (in contrast with two hydrogen bonds involving only one carboxyl oxygen in serine or a single hydrogen bond in tyrosine). The ^{13}C data of *O*-phospho-L-tyrosine **5** also deserves a short comment. The ^{13}C δ_{iso} values of the carboxyl groups for A and B conformers differ only by ca. 3.6 ppm. On the other hand, one of the δ_{22} values is much more shielded (137 ppm) than the other one (150 ppm). This must be due to some structural differences for each conformer, apparent from the analysis of molecular packing of the unit cell. The δ_{22} parameter, which is oriented close to the C═O bond, is very sensitive to such differences. We assume that δ_{22} value equal to 137 ppm corresponds to the B molecule, which is involved in weaker hydrogen bonding. Albeit the level of theory is not high enough to reproduce the same principal values of the shielding tensor as those observed experimentally, three out of

(46) (a) Stewart, J. J. P. *J. Comput. Chem.* **1989**, *10*, 209. (b) Stewart, J. J. P. *J. Comput. Chem.* **1989**, *10*, 221. (c) Jameson, C. J.; de Dios, A.; Jameson, A. K. *Chem. Phys. Lett.* **1990**, *167*, 575.
(47) Gu, Z.; McDermott, A., *J. Am. Chem. Soc.*, **1993**, *115*, 4282.
(48) Ye, C.; Fu, R.; Hu, J.; Hou, L.; Ding, S. *Magn. Reson. Chem.* **1993**, *31*, 699.

Table 4. Principal Components (in ppm) and Corresponding Anisotropic Parameters of ^{13}C and ^{31}P CSA Tensors of Carboxylic Carbon and Phosphorus Atom Calculated for *O*-Phospho-L-amino Acids Compounds

^{13}C

amino acid	data	δ_{11}	δ_{22}	δ_{33}	δ_{iso}	$\lvert\Delta\delta\rvert$	Ω	κ	η
serine	isolated	270.3	146.3	104.9	173.8	144.7	165.4	−0.5	0.4
	cluster	273.6	146.5	106.6	175.6	147.1	167.0	−0.5	0.4
	experimental	247.0	152.0	111.0	171.0	114.0	136.0	−0.4	0.5
threonine	isolated	274.5	134.6	104.6	171.2	154.9	169.9	−0.6	0.3
	cluster	260.6	171.5	104.7	178.9	122.5	155.9	−0.1	0.8
	experimental	244.0	163.0	109.0	172.0	108.0	135.0	−0.2	0.8
tyrosine	isomer A	273.6	153.1	98.8	175.2	147.7	174.8	−0.4	0.6
	isomer B	269.1	159.3	118.9	182.4	130.0	130.2	−0.5	0.5
	cluster a	265.7	136.5	103.0	168.4	146.0	162.7	−0.6	0.3
	cluster b	259.3	109.4	105.8	158.2	151.7	153.5	−1.0	0.0
	experimental	247.0	150.0	116.0	171.3	114.0	131.0	−0.5	0.4
		252.0	137.0	114.0	167.7	126.5	138.0	−0.7	0.3

^{31}P

amino acid	data	δ_{11}	δ_{22}	δ_{33}	δ_{iso}	$\lvert\Delta\delta\rvert$	Ω	κ	η
serine	isolated	98.1	5.2	−160.6	−19.1	212.3	258.7	0.3	0.7
	cluster	43.1	−21.3	−79.1	−19.1	93.3	122.2	−0.1	0.9
	experimental	51.0	4.0	−57.0	−0.9	84.5	108.0	0.1	0.8
threonine	isolated	101.1	19.5	−188.6	−22.7	248.9	289.7	0.4	0.5
	cluster	44.5	−12.8	−101.6	−23.3	117.5	146.1	0.2	0.7
	experimental	56.0	5.0	−72.0	−3.7	102.5	128.0	0.2	0.7
tyrosine	isomer A	100.2	26.0	−194.8	−22.9	257.9	295.0	0.5	0.4
	isomer B	103.6	10.6	−165.4	−17.1	222.5	269.0	0.3	0.6
	cluster A	72.5	−9.6	−126.9	−21.3	158.4	199.4	0.2	0.8
	cluster B	55.8	−11.3	−90.2	−15.2	112.5	146.0	0.1	0.9
	experimental	66.0	7.0	−86.0	−4.3	122.5	152.0	0.2	0.7
		61.0	3.0	−82.0	−5.9	114.0	143.0	0.2	0.8

[a] Isomer A corresponds to a diedral angle value of −117° for P(1A)−O(1A)−C(7A)−C(6A).[26] Isomer B corresponds to a diedral angle value of −82° for P(1B)−O(1B)−C(7B)−C(8B).[26]

four calculated $\Delta\delta$, η, Ω, and κ parameters for carboxyl groups predict that the high-field signal could be assigned to conformer B.

^{31}P Chemical Shielding Tensor in the Presence of Hydrogen Bonding. The changes of principal elements and changes in differences between them (anisotropies) are known to be more sensitive measures of hydrogen bonding than are the isotropic chemical shifts. Upon comparison of the experimental ^{31}P CSA tensor values of O-phoshorylated amino acids (Table 2), the biggest differences appear indeed for the δ_{33} element. For two conformers of **5** this parameter is equal to −82 and −86 ppm, while for **1** and **4** we have −57 and −58 ppm, respectively. Attempts were made before to correlate δ_{33} with structural parameters of a wide variety of phosphate-bearing compounds.[49] It was suggested that the observed differences of this element can reflect the changes in O═P−O valence angles or in an average length of the shortest P−O bonds. However, a lack of such correlation for our compounds means that it is not the case for O-phosphorylated amino acids and this prompted us to look for a dependence of the ^{31}P phosphoryl chemical shift tensor against the type and strength of intermolecular hydrogen bonding.

Figure 8 shows the correlation of ^{31}P δ_{ii}, $\Delta\delta$, and Ω parameters versus the intermolecular P−O···H−O−C and P−O···H−O−P hydrogen bond distance in L and DL forms of O-phosphorylated amino acids. Somewhat unexpectedly, these two groups of compounds reveal opposite trends when the hydrogen bond strength decreases; the δ_{11}, $\Delta\delta$, and Ω values increase and the δ_{33} decreases for the L form, with a reverse scenario taking place in the case of the DL form.

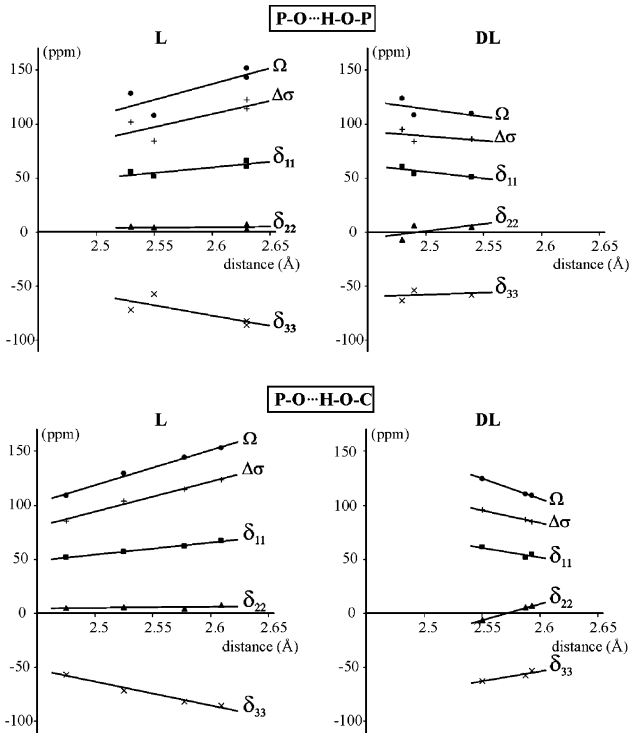

Figure 8. Plots of ^{31}P δ_{ii}, anisotropy $\Delta\delta$, and span Ω parameter versus the intermolecular P−O···H−O−C and P−O···H−O−P hydrogen bond distance in L (left) and DL (right) forms of O-phosphorylated amino acids.

The experimental observations for the L forms are in agreement with the theoretical results. Indeed, one can remark that the ^{31}P δ_{11}, $\Delta\delta$, and Ω parameters for the L forms are decreasing but δ_{33} is increasing when taking into account the

(49) Un, S.; Klein, M. P. *J. Am. Chem. Soc.* **1989**, *111*, 5119.

Table 5. Orientation of the Principal Axes of Shielding Tensor of Phosphorus Atom in O-Phosphorylated Amino Acids. For the Definition of Angles, See Figure 9

		α_1	α_{21}	α_{22}	α_{31}	α_{32}	β_1	β_2	γ	ϕ	O=P O$^-$	O(R)–P–O(H)
serine	isolated	43.7	46.0	55.5	89.7	91.4	121.4	123.7	30.8	34.4		
	cluster	57.3	33.4	69.3	94.4	97.3	111.8	130.7	22.3	43.0	114.8	101.4
	Δ^a	+13.6	−12.6	+13.8	+4.7	+5.9	−9.6	+7.0	−8.5	+8.6		
threonine	isolated	41.2	48.5	57.3	89.9	90.4	125.5	118.6	35.5	28.6		
	cluster	54.5	36.0	70.4	94.8	92.2	118.5	123.7	30.0	34.4	115.9	105.8
	Δ	+13.3	−12.5	+13.1	+4.9	+1.8	−7.0	+5.1	−5.5	+5.8		
tyrosine A	isolated	43.8	47.3	57.1	82.2	88.0	123.8	114.9	33.7	26.2		
	cluster	54.8	35.0	68.3	88.8	92.3	114.5	122.7	24.7	33.9	121.4	103.4
	Δ	+11.0	−12.3	+11.2	+6.6	+4.3	−9.3	+7.8	−9.0	+7.7		
tyrosine B	isolated	42.6	47.2	59.6	88.6	86.9	124.3	120.8	34.3	30.8		
	cluster	51.5	38.9	68.9	85.1	84.7	129.3	114.6	39.2	25.7	115.0	106.7
	Δ	+8.9	−8.3	+9.3	−3.5	−2.2	+5.0	−6.2	+4.9	−5.1		
$H_2PO_4^-$	isolated	39.2	50.3	50.6	90.8	89.5	117.0	117.0	26.9	27.1	126.0	100.9

[a] Δ = difference between angle^{isolated} and angle^{cluster}.

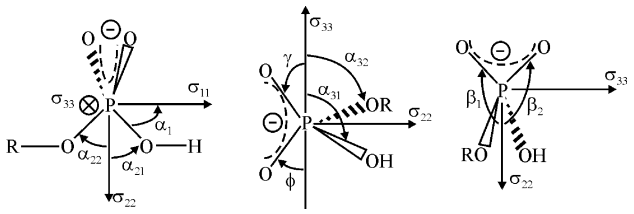

Figure 9. ^{31}P chemical shielding tensor orientation in O-phosphorylated amino acids showing three orthogonal projections of the phosphate group hydrogen bond in tyrosine.

hydrogen bonding (Table 4). This corresponds to the experimental trend of these parameters when going to stronger hydrogen bonds and has to be closely related to the orientation of chemical shielding tensor with respect to the molecular frame. In O-phoshorylated amino acids the phosphate group is involved in four hydrogen bonds linked to the O=P−O$^-$ fragment and one hydrogen bond linked to the P−OH group (except for conformer B of the tyrosine compound where the latter hydrogen bond is lacking). Figure 9 shows the orientation of ^{31}P σ_{ii} in L enantiomers of phosphorylated amino acids determined on the basis of our theoretical calculations. The relevent geometrical parameters are given in Table 5. According to Figure 9, the principal axes of the σ_{11} and σ_{22} elements lie in a plane perpendicular to the O=P−O$^-$ plane. The axis corresponding to the σ_{22} element nearly bisects the O(R)−P−O(H) angle (the sum of α_{21} and α_{22} is very close to the O(R)−P−O(H) valence angle). This axis also nearly bisects the O=P−O$^-$ angle, since the sum of β_1, β_2, and the O=P−O$^-$ angle is very close to 360°. Moreover, the values of α_{31} and α_{32} indicate that the σ_{33} axis is almost perpendicular to the O(R)−P−O(H) plane. The same axis is also in the O=P−O$^-$ plane since the sum of γ, ϕ, and the O=P−O$^-$ angle is close to 180°. This explains the most pronounced sensitivity of the ^{31}P δ_{33} element as being due to changes in the hydrogen bond strength.

Although we have not yet attempted a calculation of the shielding in DL forms of O-phoshorylated amino acids, which would confirm the opposite trends in comparison to L forms, we believe that such features have to be directly related to the different nature of the shortest hydrogen bonds. Indeed, as mentioned above, shortest hydrogen bonds in L and DL forms of phosphorylated amino acids involves respectively the carboxyl and phosphoryl groups. This implies that the phosphate residue engaged in the shortest hydrogen bond behaves as an acceptor in L forms and as a donor/acceptor in DL forms. This manifests itself by opposite changes of principal components of ^{31}P shielding tensor and of corresponding anisotropic parameters.

One has to note that the orientation of the principal axis of the ^{31}P shielding tensor in isolated molecules of O-phoshorylated amino acids is close to the orientation found in the case of the $H_2PO_4^-$ molecule. Substituting a hydrogen atom by an amino acid induces a small rotation of the σ_{11} and σ_{22} axis around the σ_{33} axis by 2−4°. Albeit the chemical shielding tensor orientation in Figure 9 is common to both types of calculations (isolated molecule or hydrogen-bonded cluster), it is clear that the presence of hydrogen bonding produces significant changes of the orientation of the shielding tensor. More specifically, as visible from α_1, α_{21}, and α_{22} values, the presence of hydrogen bonding leads to a rotation of about 12−13° around the axis of the σ_{33} element which itself rotates around the σ_{22} axis by 5−8° (see β_1, β_2 or equivalently ϕ and γ angles). One has to note that for the B conformer of O-phospho-L-tyrosine the rotation around the σ_{22} axis is reversed compared to all other molecules. We ascribe this effect to the absence of hydrogen bonding involving the P−O−H group.

Spectroscopic Distinction between Enantiomers and Racemates and Intermolecular Distances between Phosphorus Sites. In the last section, we wish to demonstrate that the study of Zeeman magnetization exchange between ^{31}P spins (with identical isotropic chemical shifts but differing chemical shielding tensor orientations) is a powerful tool for a clear distinction between enantiomers and racemate forms as well as a recognition of distinct internuclear P····P contacts in phosphorylated amino acids. For this we wish to exploit the ^{31}P proton-driven ODESSA decays shown in Figure 5. Significant differences in the rates and the amplitudes of decays are easily visible between L and DL forms. This is related to different P····P distances and a different number of contacts of exchanging nuclei. In the case of *O*-phospho-L-serine, each phosphorus atom is surrounded by the two nearest phosphorus atoms at a distance 4.71 Å. For *O*-phospho-DL-serine, only a single nearest-neighbor at distance of 4.38 Å is present, with other phosphorus atoms at longer distances (4.86, 5.95, and 6.05 Å) being related by inversion symmetry and consequently inactive in the magnetization exchange. Such subtle geometrical differences between **1** and **2** are clearly visualized by a somewhat higher amplitude but slower rate of exchange decay in **1** ($W' = 15.0\ s^{-1}$) than in **2** ($W' = 19.0\ s^{-1}$). In the case of *O*-phospho-L-threonine, each ^{31}P site is surrounded by two nearest exchanging ^{31}P sites at a

distance of 4.445 Å which leads to the spin exchange rate $W' = 20.9\ s^{-1}$. This is much more rapid than in *O*-phospho-DL-threonine, where a longer intermolecular distance between exchanging ^{31}P sites (6.21 Å, two nearest-neighbors) leads to the decay rate of $6.48\ s^{-1}$. A dramatically different situation is encountered in *O*-phospho-L-tyrosine with two crystallographically inequivalent types of phosphorus atoms P1A and P1B with different isotropic ^{31}P chemical shifts. As each phosphorus atom P1A is surrounded by four phosphorus atoms P1B, and vice versa, the spin exchange between crystallographically equivalent ^{31}P sites is much less efficient, the initial decay ($W' = 11.9\ s^{-1}$) of small amplitude results mainly from spin exchange between the crystallographically inequivalent sites. Having shown above that proton-driven ODESSA exchange experiments are very sensitive to intermolecular phosphorus−phosphorus contacts, we are now in a position to obtain structural information on O-phosphorylated DL-tyrosine of which the crystal structure is so far unknown. From a comparison of the ^{31}P spin exchange rates, we conclude that the rate ($W' = 13.0\ s^{-1}$) of spin-exchange between ^{31}P sites in **6** reveals the presence of crystallographically equivalent nearest neighbors in the distance range between 4.7 and 5.3 Å, with the longer limit corresponding to a greater number of magnetically inequivalent nearest neighbors.

Conclusions

Appropriate description and understanding of the nature of intermolecular contacts in zwitterionic, hydrogen-bonded systems of biological interest remains an important and challenging problem. In this work we have presented the first solid-state NMR study and quantum chemical calculations for a series of enantiomers and racemates of O-phosphorylated amino acids. This permitted us to determine experimentally the ^{13}C and ^{31}P principal elements of chemical shift tensors and to probe successfully the dependence of magnetic shielding on the nature and the strength of hydrogen bond contacts. Good agreement between experimental and calculated results for L forms has been obtained by the proper representation of zwitterionic isomers in the cluster type calculations. The opposite trends of principal elements of the ^{31}P shift tensor and corresponding anisotropic parameters in L and DL forms have been observed and related to the different nature of shortest hydrogen bonds involving a phosphate residue.

Significant changes in the orientation of the ^{31}P chemical shielding tensor due to the presence of hydrogen bonds have been revealed on the basis of theoretical calculations. The results obtained by these calculations constitute the first characterization of the orientation of a phosphorus chemical shielding tensor in the O-phosphorylated amino acids. Very recently, some of us have shown that solid-state ^{13}C NMR spectroscopy permits information to be obtained in a straightforward manner about the presence and the nature of all deprotonated forms of L-histidine[50a] and of malonic acid.[50b] The reliability of our ab initio calculations will permit us to use these methods for better characterization of correlations between ^{13}C and ^{31}P NMR shielding parameters and successive steps of deprotonation in O-phosphorylated amino acids as well as in several other enzymatic relevant systems.

Finally, we have also shown that in analogy to P-chiral oxazaphosphorinane derivatives,[51] by exploiting magnetization exchange betwen ^{31}P spins with differing chemical shielding tensor orientations, one can easily distinguish the enantiomers from racemates of O-phosphorylated amino acids and determine a hierarchy of long-range intermolecular distances between chemically equivalent nuclei. Such structurally relevant data may be used as valuable geometrical constraints in future quantum mechanical calculations probing molecular geometry of solids.

Acknowledgment. This work was partially supported by a research award of the Institut Nancéien de Chimie Moléculaire (INCM, FR CNRS 1742), Polish Committee for Scientific Research, KBN, Grants 3 T09A 026 19 and 4 T09A 092 22, and by the French-Polish Joint Cooperation CNRS/PAS Program 2001/2002. M.J.P. acknowledges the University Henri Poincaré, Nancy 1, for financial support. We also thank Prof. Y. Dusaussoy, University Henri Poincaré, Nancy 1, for helpful discussions.

Supporting Information Available: Table of principal components of the shielding tensor. This material is available free of charge via the Internet at http://pubs.acs.org.

JA029840Z

(50) (a) Henry, B.; Tekely, P.; Delpuech, J. J. *J. Am. Chem. Soc.* **2002**, *1124*, 2025. (b) Colsenet, R.; Gardiennet, C.; Henry, B.; Tekely, P. *Angew. Chem., Int. Ed.* **2002**, *24*, 4743

(51) Potrzebowski, M. J.; Tadeusiak, E.; Misiura, K.; Ciesielski, W.; Bujacz, G.; Tekely, P. *Chem. Eur. J.* **2002**, *8*, 5007.